Proteome of *Trichomonas vaginalis* hydrogenosome under different iron conditions

Neritza Campo Beltrán[1], Lenka Horváthová[1], Petr L. Jedelský[1,2,3], Miroslava Šedinová[1,2], Petr Rada[1], Michaela Marcinčiková[1], Ivan Hrdý[1] and Jan Tachezy[1*]

Institutions:

[1]Department of Parasitology,

Charles University in Prague, Faculty of Science, Prague, Czech Republic

[2]Laboratory of Mass Spectrometry,

Charles University in Prague, Faculty of Science, Prague, Czech Republic

[3]Department of Cell Biology,

Charles University in Prague, Faculty of Science, Prague, Czech Republic

Corresponding author:

Jan Tachezy

Charles University in Prague, Faculty of Science

Vinicna 7

12844 Prague 2

Czech Republic

Phone: +420 221 951 811

Fax: +420 224 919 704

Abstract

Limitation of iron availability is one of the principles involved in immunity. Iron plays a crucial role in metabolism as a key component of catalytic cofactors such as heme or iron sulphur clusters. Pathogens have to regulate their protein expression according to iron availability in their environment and optimize their metabolic pathways limited by availability of respective cofactors. Hydrogenosome is a mitochondrion-related organelle that harbours major pathways of energy metabolism in Trichomonas vaginalis. We analyzed hydrogenosomes obtained from control cells and cells cultivated under iron-deficient conditions employing iTRAQ, two dimensional peptide separation combining IEF and nano-HLPC with MALDI-MS/MS. We identified 634 proteins, of which 50 proteins were differentially expressed. Iron deficient conditions lead to upregulation of components involved in iron-sulfur cluster assembly and lead to downregulation of enzymes involved in carbohydrate metabolism.

Introduction

Iron is an essential element for virtually all forms of life. It plays its indispensable role as a component of metalloproteins, either bound to more or less complex prosthetic groups such as heme or iron-sulfur (FeS) clusters, or alone as e.g. in case of ribonucleotide reductase, the key enzyme of DNA metabolism. Metalloproteins are involved in many vital cellular functions including electron transport, enzymatic

catalysis, redox sensing and regulation of gene expression (Beinert et al., 1997; Sutak et al., 2008).

Trichomonas vaginalis is a sexually transmitted anaerobic parasitic protist of the Excavata group that infects man with estimated worldwide annual incidence of 170 million cases (Johnston and Mabey, 2008; WHO, 2011). One of the most prominent characteristics of this parasite is the lack of "classical" oxygen-respiring mitochondria. Instead, trichomonads possess hydrogenosomes, organelles of mitochondrial type that produce molecular hydrogen and, among other functions, synthesize ATP by substrate-level phosphorylation (Müller, 2003). Trichomonads require unusually high concentrations of iron in the in vitro cultures (Gorrell, 1985). This need has been largely attributed to the dependence of trichomonads upon the activities of FeS clusters-containing proteins that mediate the vital energy-conserving reactions in the parasite's hydrogenosomes (Vaňáčová et al., 2001), but may be also related to the fact that trichomonads apparently lack substantial levels of iron-storage proteins such as ferritin (Sutak et al., 2008) and thus high extracellular iron may be required to furnish the turnover of FeS proteins. Lactoferrin, transferrin, heme and low molecular-weight iron complexes can serve as an external source of iron for *T. vaginalis* (Sutak et al., 2008). FeS proteins involved in hydrogenosomal energy metabolism are pyruvate:ferredoxin oxidoreductase (PFO), electron carrier ferredoxin, FeFe hydrogenase and two-subunit remnant of respiratory complex 1. PFO oxidatively decarboxylates pyruvate, supplied from the cytosol or by the activity of non-FeS hydrogenosomal malic enzyme, to acetyl CoA that is converted to acetate by the activity of acetate:succinate-CoA transferase in the succinate-dependent reaction. Resulting succinyl CoA serves as a substrate for ATP

synthesis by succinate thiokinase, while electrons released from pyruvate are transported via ferredoxin to hydrogenase that forms molecular hydrogen (see Hrdý et al., 2008 for review). NADH resulting from malic enzyme reaction can be reoxidized by the complex 1 remnant (Hrdý et al., 2004). Apart from the proteins involved in hydrogenosomal carbohydrate metabolism, other hydrogenosomal Fe-containing proteins include FeS flavoproteins with unknown function, the flavodiiron oxygen reductase, peroxidase rubrerythrin, proteins of FeS cluser assembly system (Isc) of which some contain FeS clusters themselves, hybrid cluster protein, Fe superoxide dismutase and possibly others (Pütz et al., 2005; Smutna et al., 2009; Rada et al., 2011; Schneider et al., 2011).

Iron availability markedly influences hydrogenosomal catabolism, and strong upregulation of FeS enzymes involved in hydrogenosomal energy metabolism has been observed upon iron supplementation (Gorrell, 1985; Vaňáčová et al., 2001). Clearly, effective regulation linking the activity/expression of FeS proteins and the iron availability exists. Even the expression of non-FeS proteins such as one of the malic enzyme paralogs is regulated by iron via interaction of multiple nuclear Myb proteins with specific iron-responsive DNA elements (Hsu et al., 2009). The effect of iron limitation on cultivated *T. vaginalis* morphology and overall proteome changes has been studied by De Jesus et al. (2007). The cells from iron-depleted medium displayed altered morphology including internalization of flagella and axostyle and transformation to larger and rounded shape. Observed changes in protein expression included, among others, downregulation of PFO and cystein proteases, while actin was found to be upregulated in iron-depleted trichomonads (De Jesus et al., 2007) However, two dimensional gel

electrophoresis (2DE) used to separate the protein samples prior to MS identifications in the previous study is known to often fail to resolve membrane proteins, low-abundance proteins, proteins with extreme pI values and also very small or large ones (Nägele et al., 2004), resulting in incomplete list of identified proteins potentially including those affected by changes in external conditions. Our previous experiments showed that hydrogenosomes contain majority of proteins with basic pI and that major metabolic enzymes such as malic enzyme cross-contaminate other spots and thus hamper identifications from 2DE. Therefore, in this report describing the changes in the expression of hydrogenosomal proteins in response to iron limitation we utilized gel-free approach based on iTRAQ, isoelectric focusing of tryptic peptides and nano LC-MALDI identification. We focused specifically on hydrogenosomes, because many FeS proteins reside in these organelles along with the FeS cluster assembly system. To maximize the specificity and sensitivity of our approach, we used highly purified hydrogenosomes.

Methods

Parasite cultivation

Trichomonas vaginalis strain T1 (J.H. Tai, Institute of Biomedical Sciences, Taipei, Taiwan) was grown in Diamond´s trypticase-yeast-extract-maltose (TYM medium) supplemented with 10% heat-inactivated horse serum without agar at pH 6,2 (Diamond, 1957). The iron-supplemented medium was prepared by adding ammonium ferric citrate to a final iron concentration of 86 μM. Iron-restricted cells were subcultured for 10 passages in iron-deficient TYM medium prepared without ammonium ferric citrate and

by adding 2,2´-dipyridyl (Sigma Chemical Co., St. Louis, Missouri) to a final concentration of 70 μM.

Cell fractionation and isolation of hydrogenosomes

One liter of cultures of *T. vaginalis* cells grown in iron enriched (+Fe) and iron depleted (-Fe) conditions were harvested by centrifugation at 1300×g for 12 min. at 4°C and washed twice with 50 ml of phosphate buffered saline (PBS) and once with 50 ml of isotonic ST buffer (250 mM sucrose, 10 mM Tris, 0,5 mM KCl, pH 7.2). Subsequent steps were performed at 4°C in ST buffer supplemented with protease inhibitors TLCK 50 μg/ml (Tosyl Lysyl Chloromethyl Ketone) and Leupeptin 10 μg/ml (N-acetyl-L-leucyl-L-leucyl-L-argininal). Cell pellets were resuspended in 40 ml of ST buffer and sonicated on ice until approximately 80-90% of the cells were disrupted. The homogenate was centrifuged at 800×g for 15 minutes to remove the nuclei and unbroken cells. The supernatant was centrifuged at 17000×g for 20 minutes resulting in an enriched large granular fraction (LGF,sediment) and crude cytosolic fraction (supernatant). In order to obtain highly purified hydrogenosomes, the enriched LGF was further fractionated using discontinuous Optiprep^{tm} gradient (Axis-Shield). To prepare the gradient, 0.5 ml of 50% (w/v) Optiprep working solution was applied to the bottom of the tube and 1 ml of each lower-density solution (ranging from 36 to 18% in 2%steps) was layered successively. The Optiprep working solution was prepared by diluting the original Optiprep^{tm} to the concentration of 50% using a diluent recommended for general purposes (0.25 M sucrose, 6 mM EDTA, 60 mM Tris-HCl, pH 7.4). Successive gradient solutions were prepared by diluting the 50% working solution with the homogenization buffer (0.25 M

sucrose, 1 mM EDTA, 10 mM Tris-HCl, pH 7.4) to the specific concentration. The LGF was resuspended in 0.5 ml of homogenization buffer and layered on the top of the gradient. The gradient was centrifuged in swinging bucket rotor at 200000×g for 2 hours at 4°C. The separated fractions were then carefully removed using a micropipette and each fraction was washed separately with ST buffer containing protease inhibitors at 21000×g for 20 minutes at 4°C.

SDS-PAGE and Western Blotting

SDS-PAGE and Western blotting were used to analyze the protein composition of Optiprep-sucrose purified hydrogenosomes. SDS-PAGE was performed on a Bio-Rad miniprotean gel apparatus using 12% gel. Electrophoretically resolved proteins were stained with Coomassie brilliant blue or transferred to a nitrocellulose transfer membrane to be probed by polyclonal rabbit antiserum against hydrogenosomal malic enzyme (Drmota et al., 1996).

Transmission Electron Microscopy (TEM)

Pellets of each fraction obtained from the Optiprep-sucrose gradients were fixed for 24 h in 2,5% glutaraldehyde in 0,1M cacodylate buffer (pH 7,2) and postfixed in 2% OsO_4 in the same buffer. Fixed specimens were dehydrated through an ascending ethanol and acetone series and embedded in Araldite - Poly/Bed® 812 resin mixture. Thin sections were cut on a Reichert-Jung Ultracut E ultramicrotome and stained using uranyl acetate and lead citrate. Sections were examined and photographed using JEOL JEM-1011

electron microscope with Megaview III camera and analySIS 3.2 software (Soft Imaging System®).

Determination of enzymatic activities

Activities of hydrogenosomal and non-hydrogenosomal enzymes were measured spectrophotometrically at 25°C in all fractions. Hydrogenosomal malic enzyme was measured aerobically at 340 nm as the rate of malate dependent NAD^+ reduction (Drmota et al., 1996) and the lysosomal marker enzyme acid phosphatase was measured according to Barret (1972). The activity determinations were carried out immediately after organelle isolation. Protein concentrations in the fractions were determined by the Lowry method (Lowry et al., 1951).

Protein digestion and iTRAQ labelling

Aliquots of hydrogenosomal fractions containing 100µg of total protein were precipitated with 300 µl of acetone overnight at -20°C. The precipitate was centrifuged, acetone was carefully poured out and the rest of acetone was left to evaporate for 5 minutes. Sample dissolution, reduction, alkylation, digestion and iTRAQ 4-plex labelling were performed according to the manufacturer´s instructions (AB Sciex, Foster City, CA) using sequencing grade porcine trypsin (Promega). Combined samples were precipitated with 500 µl of acetone overnight at -20°C. The precipitate was centrifuged, acetone was carefully poured out and the rest of acetone was left to evaporate for 5 minutes.

Isoelectric focusing, extraction and HPLC

Combined iTRAQ labelled sample was dissolved in 250 µl of 2 M urea and poured to 17cm long focusing tray of Protean IEF Cell (Bio-Rad, Hercules, CA, USA). Sample was covered with 17cm IPG strips (pH 3-10, Bio-Rad) without paper wicks and oil. Active rehydration at 50 V for 2 hours was followed by voltage steps 100, 250, 500 and1000 for 15 minutes and maximum of 10 kV until 40 kVHrs were reached. Final step comprised 500 V forever. Current was limited to 50 µA and only one strip was focused at a time. Strip was cut into pieces approximately 2-3mm wide. These pieces were in parallel sonicated for 15 minutes with 20 µl of 50% acetonitrile (ACN) with 0.1% trifluoroacetic acid. Supernatants were mixed 1:1 with water and subjected to nano-reversed phase HPLC. LC-MALDI analyses were performed on Ultimate 3000 HPLC system (Dionex, Framingham, MA) coupled to Probot micro-fraction collector (Dionex). Extracted post-IEF fractions were loaded onto a PepMap 100 C18 RP column (3 µm particle size, 15cm long, 75 µm internal diameter; Dionex) and separated by a gradient of 5% (v/v) acetonitrile, 0.1% (v/v) trifluoroacetic acid to 80% (v/v) acetonitrile, 0.1% (v/v) trifluoroacetic acid over a period of 60 min. The flow rate was set to 300 nl/min. Eluate was mixed 1:3 with matrix solution (2 mg/ml α-cyano-4-hydroxycinnamic acid in 80% ACN) by Probot micro-fraction spotter prior to spotting onto a MALDI target. Spotting frequency was 5 spots per minute, i.e. 60 nl eluate + 180 nl matrix solution per MALDI spot.

Mass spectrometry

Spectra were acquired on 4800 Plus MALDI TOF/TOF analyzer (AB Sciex) equipped with a Nd:YAG laser (355 nm, firing rate 200 Hz). All spots were first measured in MS

mode from m/z 800 to 4,000 and then up to 15 strongest precursors were selected for MS/MS analysis, which was performed with 1 kV collision energy and operating pressure of collision cell set to 10^{-6} Torr. Tandem mass spectra were processed with 4000 Series Explorer with subtract baseline enabled (peak width 50), Gaussian smoothing was applied with filter width 5, minimum signal to noise 8, local noise window width 250 m/z, minimum peak width at full width half max 2.9 bins, cluster area signal to noise optimization enabled (threshold 15), flag monoisotopic peaks enabled (generic formula C_6H_5NO).

Proteomic data analysis

Database search was performed with GPS Explorer v. 3.6 (AB Sciex) with locally installed Mascot v. 2.1 (Matrix Science) against database of *Trichomonas vaginalis* annotated protein sequences from TrichDB (http://trichdb.org) release-1.2, 21-Sep-2010, 119344 sequences) with trypsin digestion, methyl methanethiosulfonate modification of cysteines, N-terminal and ε-amino group of lysine modified with iTRAQ 4-plex reagents as fixed modifications and methionine oxidation as variable modification. Precursor tolerance was set 100 ppm and MS/MS fragment tolerance 0.2 Da. Maximum peptide rank was 1 and minimum ion score C.I. per peptide was 95%. Spectra assigned to more than one protein were not used for quantitation. Average iTRAQ ratios and standard deviations were calculated for each protein using all available treatment/control iTRAQ pairs.

Results and Discussion

Idetification of hydrogenosomal proteins by mass spectrometry

To investigate changes of *T. vaginalis* hydrogenosomal proteome caused by iron limitation, trichomonads were grown in media supplemented with 70 μM iron chelator 2,2-dipyridyl (iron-restricted conditions, -Fe). As a control we used trichomonads grown in media supplemented with ammonium ferric citrate to a final iron concentration of 86 μM (iron-rich conditions, +Fe). Highly purified hydrogenosomes were obtained from homogenates of both cultures by differential centrifugation followed by preparative centrifugation of large granular fraction using a discontinuous Optiprep (iodixanol) gradient. In both iron conditions ten organellar fractions apparent as cloudy bands with variable thickness and density were obtained. The band appearance/distribution somewhat differed between +Fe and -Fe conditions (Figure 1). Western blot analyses of fractions showed that the hydrogenosomal marker malic enzyme is particularly enriched in fractions #7 and #8 in iron-rich (+Fe), and in fractions #6 and #7 in iron-depleted (-Fe) conditions (Figure 2). The purity of fractions was further examined by electron microscopy (Figure 3) and by determination of enzymatic activities of hydrogenosomal and lysosomal markers malic enzyme and acid phosphatase, respectively (Figure 4). Based on the combination of these results, fraction #7 appeared to be the most pure hydrogenosomal fraction with the least contamination and was therefore chosen for comparative proteomic analysis.

Proteins of this fraction were digested and labeled using iTRAQ 4-plex kit. The labeled peptides were fractionated using isoelectric fractionation focusing and analyzed using LC-MS/MS. Five independent biological replicates were included in the analysis.

Two pairs of biological replicates were processed and measured in two iTRAQ -LC-MS analyses and one pair was measured in a separate analysis. In total we acquired over 64 000 MS/MS spectra in 200 LC runs. Mascot 2.1 search engine identified a total of 634 proteins (Table S1). Spectra assigned to more than one protein were not used for quantitation. Average ratio for each protein was calculated from all available iTRAQ pairs. Only values calculated using at least three pairs (thus at least from two spectra) were taken. Proteins with average ratio at least ±2.0 were considered as differentially expressed.

In order to distinguish hydrogenosomal proteins from contamination four different bioinformatic tools for the prediction of subcellular localization (PSORT II, ProtComp v. 9.0, Euk-mPLoc 2.0 and Yloc) were used. The protein was considered to be putatively hydrogenosomal if mitochondrial localization was predicted by at least one of the tools. This prediction, which yielded 299 putative hydrogenosomal proteins (Table S2), was further refined using (i) BlastP to reveal proteins annotated in other metabolic pathways (ii) a Java application that specifically searched for the proteins containing N-terminal hydrogenosomal presequences (Šmíd et al., 2008). This approach selected 149 proteins with highly probable hydrogenosomal localization that are members of eight different functional categories (Table 1).

Altogether 49 proteins met criteria for iTRAQ ratio and putative hydrogenosomal localization, 24 of them where upregulated while 25 were downregulated in iron deficient conditions (Table2).

Iron sulfur cluster assembly

Hydrogenosomes of *T. vaginalis* possess machinery required for the formation of FeS clusters that is homologous to the mitochondrial ISC system. (Sutak et al., 2004; Hjort et al., 2010). Iron depletion caused increased expression of almost all known components involved in hydrogenosomal ISC assembly machinery, yet some of them did not reach the cut off limit (Figure 5, Table 1). Significantly upregulated were all three detected homologues of the scaffold protein IscA-2 as well as four detected copies of the Nfu scaffolds, however, expression of IscU, which is believed to act as a principal scaffold, did not show iron dependent regulation (Table 2). This may suggest that *Trichomonas* uses alternative scaffolds IscA or Nfu instead of IscU. Unlike in mitochondria, which possess two types of IscA homologues (Isa1 and Isa2), only IscA-2 encoding genes were identified in *T. vaginalis* genome (Carlton et al., 2007). Mitochondrial Isa1 and Isa2 are, together with Iba57, specifically required for the maturation of aconitase and activation of SAM enzymes (Gelling et al., 2008). In hydrogenosomes, no aconitase is present, nevertheless a SAM enzyme HydE is essential for hydrogenase maturation (Putz et al., 2006; see below). Therefore, one more anticipated function of hydrogenosomal IscA-2 might be in the activation of HydE. Another protein that most likely fulfils the function of a scaffold is P-loop NTPase Ind1, which is in mitochondria specifically required for the assembly of respiratory complex I (Bych et al., 2008). Four homologues of Ind1 were detected in the hydrogenosomal proteome, which correlates with the presence of a reduced (two subunit) form of complex I within the organelle (Hrdý et al., 2004). One of the proteins was significantly upregulated in -Fe conditions. Similarly a single homologue of Isd11, an accessory

protein of cysteine desulfurase (IscS) (Pandey et al., 2011), was significantly upregulated under -Fe conditions, while the upregulation of the second detected copy of this protein as well as of IscS itself was not significant. Consistently with the previous study of Sutak et al. (2004) our study detected only IscS-2, while IscS-1 was not found, suggesting that only one of the two gene copies is expressed. Of the components that act late in the FeS proteins biogenesis and ensure the transfer of the nascent FeS cluster to the target apoprotein, two homologues of the chaperone HSP70 and one nucleotide exchange factor Mge1 (GrpE), were significantly upregulated in -Fe conditions.

Hydrogenosomal Hyd machinery that consists of three proteins HydE, HydF and HydG is essential for the maturation of the H cluster, the active site of FeFe hydrogenase (Putz et al., 2006; Mulder et al., 2010). Interestingly, one homologue of each component was upregulated in -Fe, and moreover HydG showed the highest fold change between the two iron conditions (Table 2).

Based on the overall upregulation of ISC components under iron limitation a common mechanism of expression regulation can be expected. Multifarious Myb-like regulatory machinery was shown to regulate iron-dependent expression of malic enzyme; one of the identified myb regulatory element was named MRE2f (Ong et al., 2006, 2007; Hsu et al., 2009). In our recent study, we have found the MRE2f motif in the 5'untranslated regions of IscS (TVAG_239660) and IscA2 (TVAG_456770)(Horváthová et al., in press), suggesting that regulation of these genes might be accomplished through the Myb system. However, the mode of regulation of the rest of ISC components remains unclear.

Energy metabolism

Iron restriction resulted in decreased expression of all enzymes involved in hydrogenosomal carbohydrate metabolism. These enzymes are in *T. vaginalis* coded by multiple genes; our analysis detected virtually all gene products (Figure 6, Table1), however only one or several homologues of a particular enzyme were significantly downregulated (Table2). Two crucial FeS enzymes of the pathway, PFO and FeFe hydrogenase, as well as a non-FeS malic enzyme were among the most downregulated proteins. Three homologues of PFO displayed downregulation one order of magnitude bigger than those obtained for the rest of regulated proteins (fold changes -37.4, -16.9 and -13.5). Only one of all detected homologues was significantly downregulated in following cases: both subunits of the remnant respiratory complex I, acetate:succinate-CoA transferase (ASCT) and heterodimeric succinate thiokinase (STK), of which only the α subunit showed significant downregulation in -Fe conditions.

Seven homologues of ferredoxin (Fdx) ensure transport of electrons in *T. vaginalis* hydrogenosomes. Three of the homologues showed significant and one nonsignificant downregulation in -Fe conditions, while three homologues appear to be upregulated, albeit their fold changes did not reach the cut off limit (Table 1). It could be speculated that Fdxs share the trend of regulation with the pathway in which they are involved. Therefore we suggest that downregulated Fdx homologues are involved in the energy metabolism, while those that are upregulated participate in the ISC assembly.

Oxygen detoxification system

Although *T. vaginalis* inhabits oxygen poor environment, it must possess defense mechanisms to protect itself, and particularly oxygen-sensitive hydrogenosomal enzymes PFO and hydrogenase, against oxygen and reactive oxygen species (ROS). The spectrum of proteins that can play a role in hydrogenosomal oxygen detoxification system seems to be unexpectedly broad (Coombs et al., 2004; Pütz et al., 2005; Schneider et al., 2011). We have detected five proteins possibly involved in oxygen and ROS defence , expression of which was significantly influenced by iron availability (Table 2).

References

Beinert, H., Holm, R. H., and Münck, E. (1997). Iron-sulfur clusters: nature's modular, multipurpose structures. Science (New York, N.Y.) *277*, 653–659.

Bych, K., Kerscher, S., Netz, D. J. A., Pierik, A. J., Zwicker, K., Huynen, M. A., Lill, R., Brandt, U., and Balk, J. (2008). The iron-sulphur protein Ind1 is required for effective complex I assembly. The EMBO journal *27*, 1736–1746.

Carlton, J. M., Hirt, R. P., Silva, J. C., Delcher, A. L., Schatz, M., Zhao, Q., Wortman, J. R., Bidwell, S. L., Alsmark, U. C. M., Besteiro, S., et al. (2007). Draft genome sequence of the sexually transmitted pathogen Trichomonas vaginalis. Science (New York, N.Y.) *315*, 207–212.

Coombs, G. H., Westrop, G. D., Suchan, P., Puzova, G., Hirt, R. P., Embley, T. M., Mottram, J. C., and Muller, S. (2004). The amitochondriate eukaryote Trichomonas vaginalis contains a divergent thioredoxin-linked peroxiredoxin antioxidant system. J.Biol.Chem. *279*, 5249–5256.

Diamond, L. S. (1957). The establishment of various trichomonads of animals and man in axenic cultures. J.Parasitol. *43*, 488–490.

Drmota, T., Proost, P., Weyda, F., Ranst, M. V., Kulda, J., and Tachezy, J. (1996). Iron-ascorbate cleavable malic enzyme from hydrogenosomes of Trichomonas vaginalis: purification and characterization. Molecular and Biochemical Parasitology *83*, 221–234.

Gelling, C., Dawes, I. W., Richhardt, N., Lill, R., and Mühlenhoff, U. (2008). Mitochondrial Iba57p is required for Fe/S cluster formation on aconitase and activation of radical SAM enzymes. Molecular and cellular biology *28*, 1851–1861.

Gorrell, T. E. (1985). Effect of culture medium iron content on the biochemical composition and metabolism of Trichomonas vaginalis. Journal of bacteriology *161*, 1228–1230.

Hjort, K., Goldberg, A. V., Tsaousis, A. D., Hirt, R. P., and Embley, T. M. (2010). Diversity and reductive evolution of mitochondria among microbial eukaryotes. Philos.Trans.R.Soc. B *365*, 713–727.

Horváthová, L., Šafaříková, L., Basler, M., Hrdý, I., Beltrán, N. C., Shin, J.-W., Huang, K.-Y., Huang, P.-J., Lin, R., Tang, P., et al. (2012). A transcriptome analysis reveals iron-regulated genes in Trichomonas vaginalis. Int.J.Parasitol.

Hrdy, I., Hirt, R. P., Dolezal, P., Bardonova, L., Foster, P. G., Tachezy, J., and Embley, T. M. (2004). Trichomonas hydrogenosomes contain the NADH dehydrogenase module of mitochondrial complex I. Nature *432*, 618–622.

Hrdý, I., Tachezy, J., and Müller, M. (2008). Metabolism of Trichomonad Hydrogenosomes. In Hydrogenosomes and Mitosomes: Mitochondria of Anaerobic Eukaryotes, J. Tachezy, ed. (Berlin: Heidelberg: Springer-Verlag), pp. 113–144.

Hsu, H. M., Ong, S. J., Lee, M. C., and Tai, J. H. (2009). Transcriptional regulation of an iron-inducible gene by differential and alternate promoter entries of multiple Myb proteins in the protozoan parasite Trichomonas vaginalis. Eukaryot.Cell *8*, 362–372.

De Jesus, J. B., Cuervo, P., Junqueira, M., Britto, C., Silva-Filho, F. C. E., Soares, M. J., Cupolillo, E., Fernandes, O., and Domont, G. B. (2007). A further proteomic study on the effect of iron in the human pathogen Trichomonas vaginalis. Proteomics *7*, 1961–1972.

Johnston, V. J., and Mabey, D. C. (2008). Global epidemiology and control of Trichomonas vaginalis. Current opinion in infectious diseases *21*, 56–64.

Lowry, O. H., Rosebrough, N. J., Farr, A. L., and Randall, R. J. (1951). Protein measurement with the Folin phenol reagent. The Journal of biological chemistry *193*, 265–275.

Mulder, D. W., Boyd, E. S., Sarma, R., Lange, R. K., Endrizzi, J. a, Broderick, J. B., and Peters, J. W. (2010). Stepwise [FeFe]-hydrogenase H-cluster assembly revealed in the structure of HydA(DeltaEFG). Nature *465*, 248–251.

Muller, M. (2003). Energy metabolism Part I: Anaerobic protozoa . In Molecular medical parazitology , J. J. Marr, T. W. Nilsen, and R. W. Komuniecky, eds. (New York : Academic Press), pp. 125–139.

Nägele, E., Vollmer, M., Hörth, P., and Vad, C. (2004). 2D-LC/MS techniques for the identification of proteins in highly complex mixtures. Expert review of proteomics *1*, 37–46.

Ong, S. J., Hsu, H. M., Liu, H. W., Chu, C. H., and Tai, J. H. (2007). Activation of multifarious transcription of an adhesion protein ap65-1 gene by a novel Myb2 protein in the protozoan parasite Trichomonas vaginalis. J.Biol.Chem. *282*, 6716–6725.

Ong, S. J., Hsu, H. M., Liu, H. W., Chu, C. H., and Tai, J. H. (2006). Multifarious transcriptional regulation of adhesion protein gene ap65-1 by a novel Myb1 protein in the protozoan parasite Trichomonas vaginalis. Eukaryot.Cell *5*, 391–399.

Pandey, A., Yoon, H., Lyver, E. R., Dancis, A., and Pain, D. (2011). Isd11p protein activates the mitochondrial cysteine desulfurase Nfs1p protein. The Journal of biological chemistry *286*, 38242–38252.

Putz, S., Dolezal, P., Gelius-Dietrich, G., Bohacova, L., Tachezy, J., and Henze, K. (2006). Fe-hydrogenase maturases in the hydrogenosomes of Trichomonas vaginalis. Eukaryot.Cell *5*, 579–586.

Pütz, S., Gelius-Dietrich, G., Piotrowski, M., and Henze, K. (2005). Rubrerythrin and peroxiredoxin: two novel putative peroxidases in the hydrogenosomes of the microaerophilic protozoon Trichomonas vaginalis. Molecular and biochemical parasitology *142*, 212–223.

Rada, P., Doležal, P., Jedelský, P. L., Bursac, D., Perry, A. J., Šedinová, M., Smíšková, K., Novotný, M., Beltrán, N. C., Hrdý, I., et al. (2011). The core components of organelle biogenesis and membrane transport in the hydrogenosomes of Trichomonas vaginalis. PloS one *6*, e24428.

Schneider, R. E., Brown, M. T., Shiflett, A. M., Dyall, S. D., Hayes, R. D., Xie, Y., Loo, J. a, and Johnson, P. J. (2011). The Trichomonas vaginalis hydrogenosome proteome is highly reduced relative to mitochondria, yet complex compared with mitosomes. International journal for parasitology *41*, 1421–1434.

Smutna, T., Goncalves, V. L., Saraiva, L. M., Tachezy, J., Teixeira, M., and Hrdy, I. (2009). Flavodiiron protein from Trichomonas vaginalis hydrogenosomes: the terminal oxygen reductase. Eukaryot.Cell *8*, 47–55.

Smíd, O., Matusková, A., Harris, S. R., Kucera, T., Novotný, M., Horváthová, L., Hrdý, I., Kutejová, E., Hirt, R. P., Embley, T. M., et al. (2008). Reductive evolution of the mitochondrial processing peptidases of the unicellular parasites trichomonas vaginalis and giardia intestinalis. PLoS pathogens *4*, e1000243.

Sutak, R., Dolezal, P., Fiumera, H. L., Hrdy, I., Dancis, A., Delgadillo-Correa, M., Johnson, P. J., Muller, M., and Tachezy, J. (2004). Mitochondrial-type assembly of FeS centers in the hydrogenosomes of the amitochondriate eukaryote Trichomonas vaginalis. Proc.Natl.Acad.Sci.U.S.A *101*, 10368–10373.

Sutak, R., Lesuisse, E., Tachezy, J., and Richardson, D. R. (2008). Crusade for iron: iron uptake in unicellular eukaryotes and its significance for virulence. Trends Microbiol. *16*, 261–268.

Vanácová, S., Rasoloson, D., Rázga, J., Hrdý, I., Kulda, J., and Tachezy, J. (2001). Iron-induced changes in pyruvate metabolism of Tritrichomonas foetus and involvement of iron in expression of hydrogenosomal proteins. Microbiology *147*, 53–62.

World health organisation (2011). Global Prevalence and incidence of Selected Curable Sexually Transmitted Infections. Available at: http://www.who.int/docstore/hiv/GRSTI/006.htm.

Figure legends

Figure 1. Optiprep density gradient fractionation. *Trichomonas vaginalis* cells were grown in iron rich and iron depleted media, harvested, disrupted by sonication and centrifuged to remove unbroken cells and nuclei. The large granular fraction was layered onto an Optiprep density gradient. Ten distinct fractions were obtained.

Figure 2. SDS-PAGE and western blot analysis of Optiprep density gradient fractions. Fractions colleted from Optiprep density gradient were analyzed by SDS-PAGE and western blot with polyclonal rabbit antiserum against hydrogenosomal malic enzyme.

Figure 3. Electron microscopy of subcellular fractions.

Figure 4. Enzyme activities in subcellular fractions. (A) Malic enzyme and (B) acid phosphatase activity in subcellular fractions from Optiprep density gradient from control (black bars) and iron depleted sample (red bars).

Figure 5. Differentially expressed components of iron sulphur cluster assembly machinery.

Figure 6. Differentially expressed components of hydrogenosomal energy metabolism pathways.

Figure 1

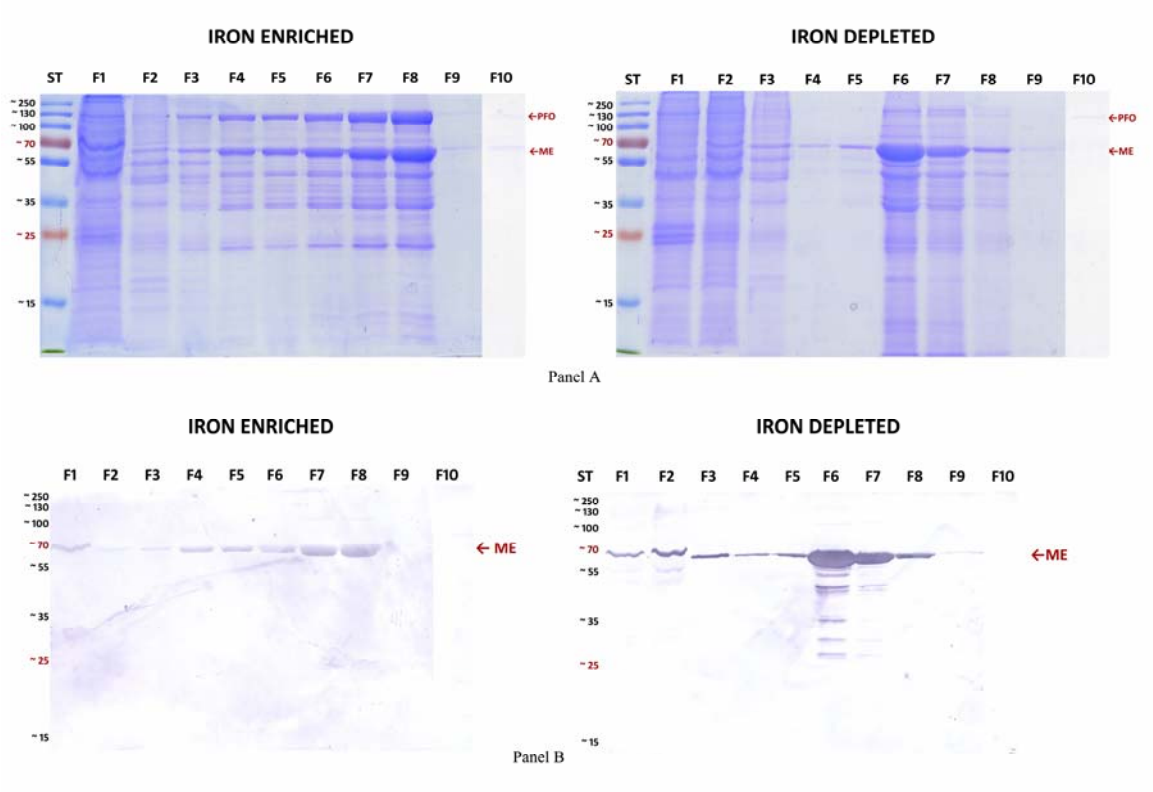
IRON ENRICHED
IRON DEPLETED
ST F1 F2 F3 F4 F5 F6 F7 F8 F9 F10
~250
~130
~100
~70
~55
~35
~25
~15
←PFO
←ME
Panel A
IRON ENRICHED
IRON DEPLETED
F1 F2 F3 F4 F5 F6 F7 F8 F9 F10
ST F1 F2 F3 F4 F5 F6 F7 F8 F9 F10
← ME
←ME
Panel B

Figure 2

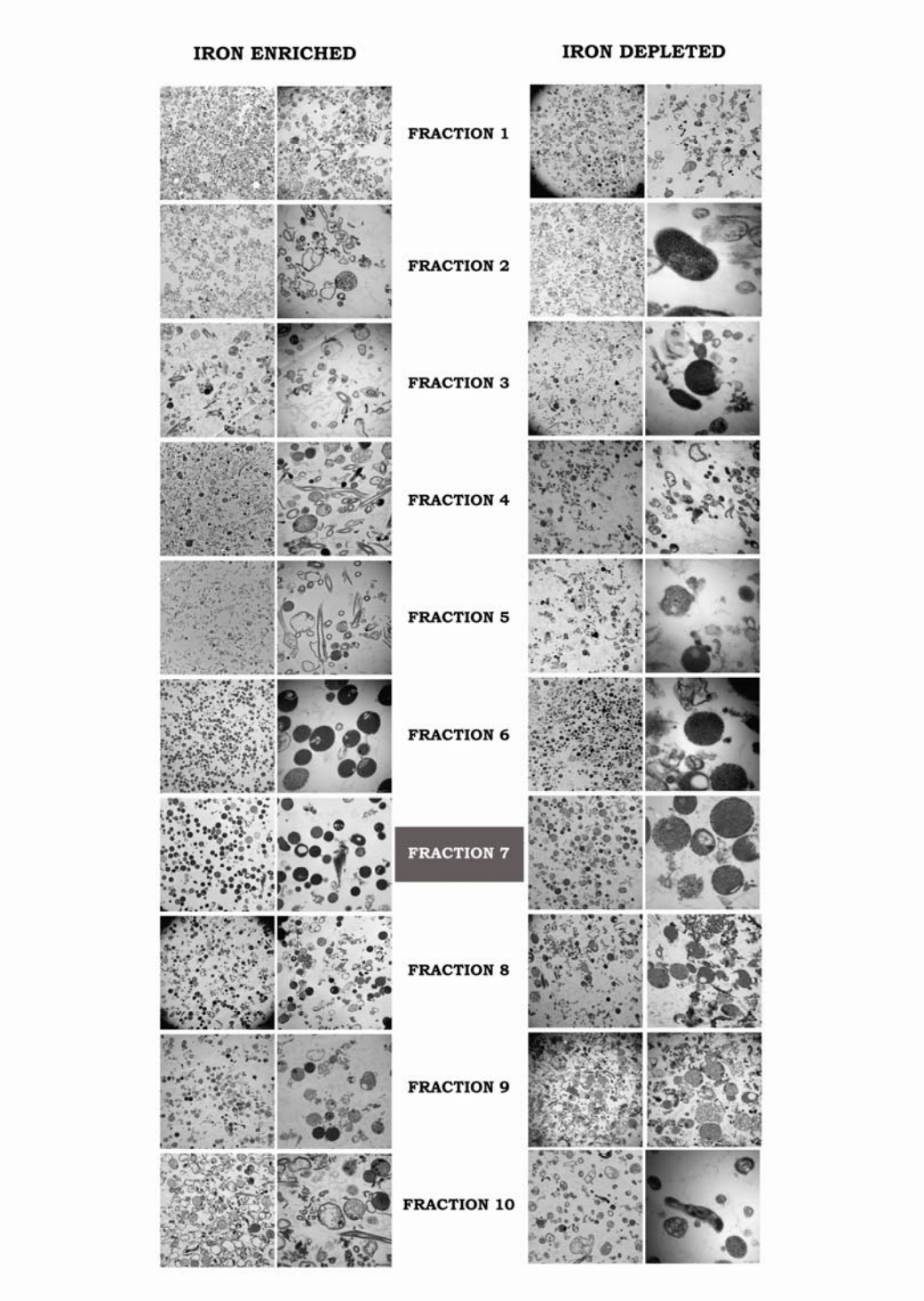
IRON ENRICHED
IRON DEPLETED
FRACTION 1
FRACTION 2
FRACTION 3
FRACTION 4
FRACTION 5
FRACTION 6
FRACTION 7
FRACTION 8
FRACTION 9
FRACTION 10

Figure 3

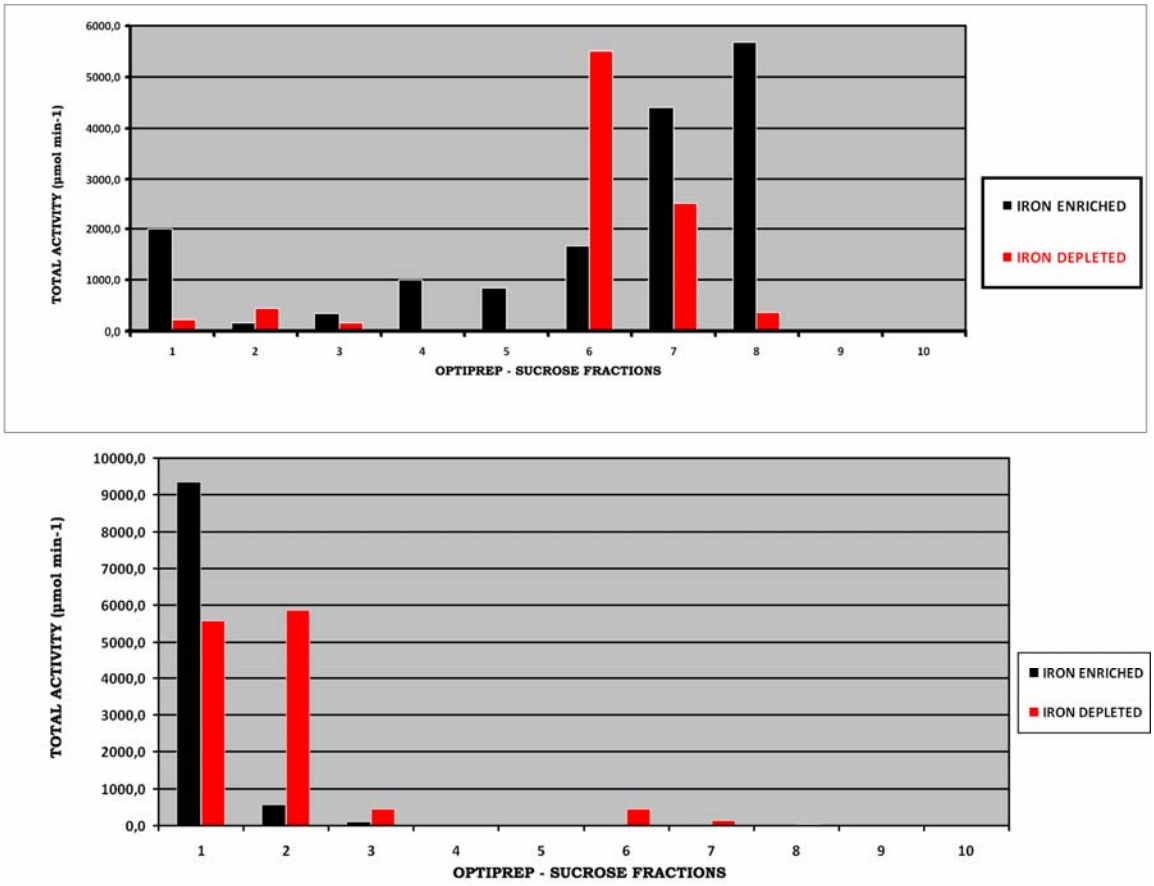
6000,0
5000,0
4000,0
3000,0
2000,0
1000,0
0,0
TOTAL ACTIVITY (µmol min-1)
1
2
3
4
5
6
7
8
9
10
OPTIPREP - SUCROSE FRACTIONS
IRON ENRICHED
IRON DEPLETED
10000,0
9000,0
8000,0
7000,0
6000,0
5000,0
4000,0
3000,0
2000,0
1000,0
0,0
TOTAL ACTIVITY (µmol min-1)
1
2
3
4
5
6
7
8
9
10
OPTIPREP - SUCROSE FRACTIONS
IRON ENRICHED
IRON DEPLETED

Figure 4

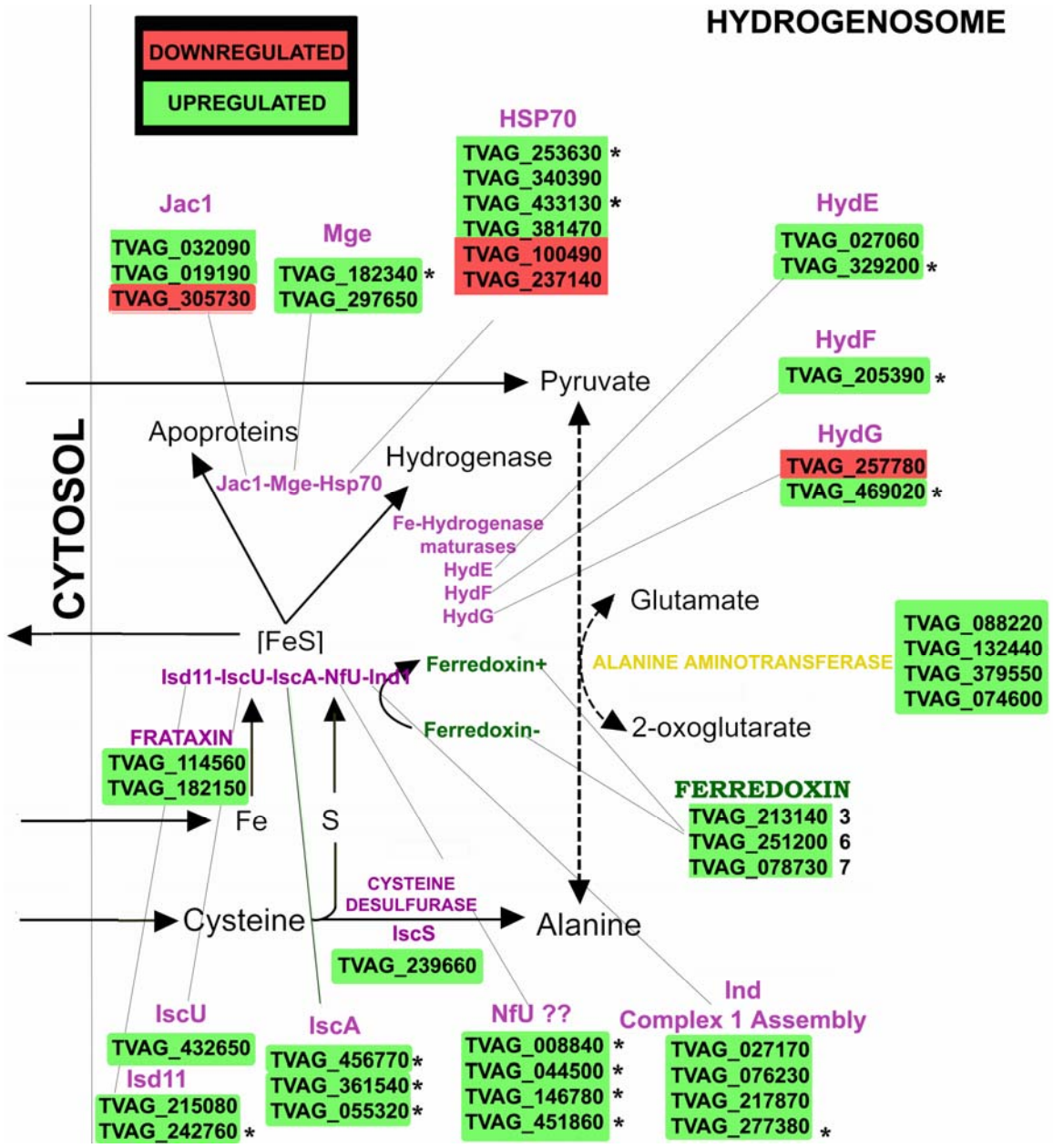
HYDROGENOSOME
DOWNREGULATED
UPREGULATED
HSP70
TVAG_253630 *
TVAG_340390
TVAG_433130 *
TVAG_381470
TVAG_100490
TVAG_237140
Jac1
TVAG_032090
TVAG_019190
TVAG_305730
Mge
TVAG_182340 *
TVAG_297650
HydE
TVAG_027060
TVAG_329200 *
HydF
TVAG_205390 *
HydG
TVAG_257780
TVAG_469020 *
Pyruvate
CYTOSOL
Apoproteins
Hydrogenase
Jac1-Mge-Hsp70
Fe-Hydrogenase
maturases
HydE
HydF
HydG
Glutamate
[FeS]
Ferredoxin+
Isd11-IscU-IscA-NfU-Ind1
ALANINE AMINOTRANSFERASE
TVAG_088220
TVAG_132440
TVAG_379550
TVAG_074600
Ferredoxin-
2-oxoglutarate
FRATAXIN
TVAG_114560
TVAG_182150
FERREDOXIN
TVAG_213140 3
TVAG_251200 6
TVAG_078730 7
Fe
S
CYSTEINE
DESULFURASE
Cysteine
Alanine
IscS
TVAG_239660
Ind
Complex 1 Assembly
IscU
TVAG_432650
IscA
TVAG_456770*
TVAG_361540*
TVAG_055320*
NfU ??
TVAG_008840 *
TVAG_044500 *
TVAG_146780 *
TVAG_451860 *
TVAG_027170
TVAG_076230
TVAG_217870
TVAG_277380 *
Isd11
TVAG_215080
TVAG_242760 *

Figure 5

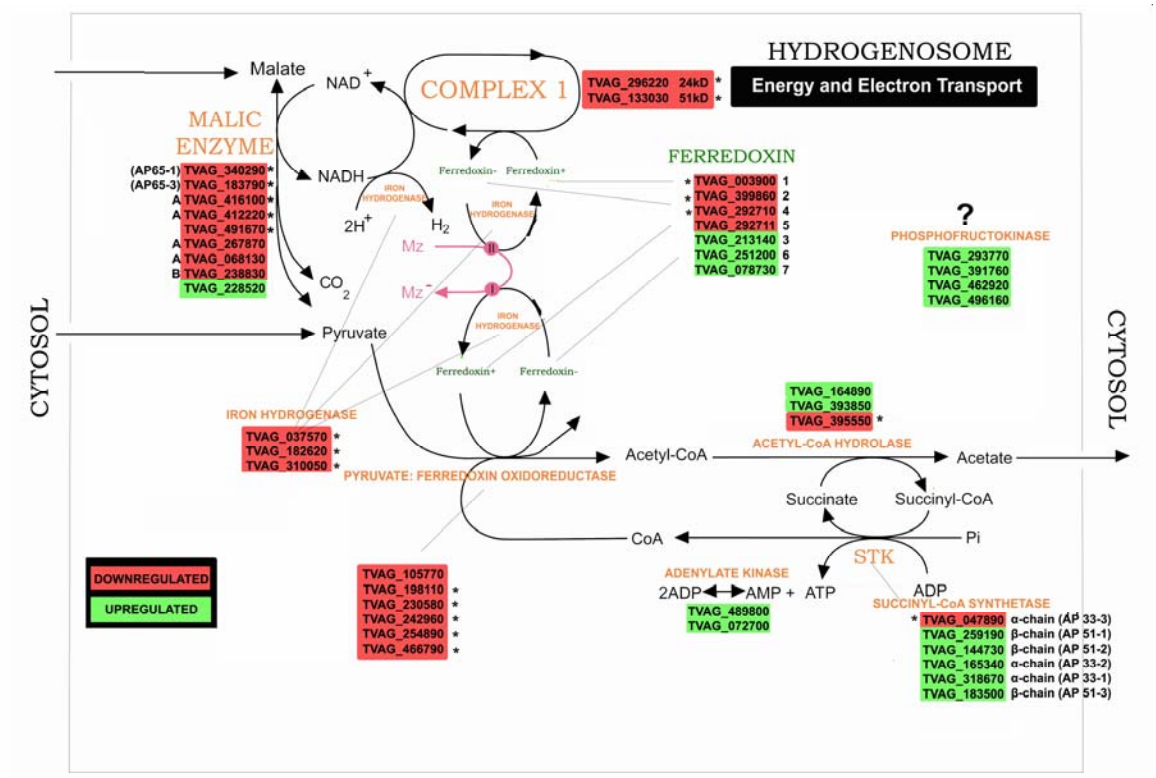
HYDROGENOSOME
Energy and Electron Transport
Malate
NAD +
COMPLEX 1
TVAG_296220 24kD *
TVAG_133030 51kD *
MALIC ENZYME
(AP65-1) TVAG_340290 *
(AP65-3) TVAG_183790 *
A TVAG_416100 *
A TVAG_412220 *
TVAG_491670 *
A TVAG_267870
A TVAG_068130
B TVAG_238830
TVAG_228520
NADH
2H+
H2
CO2
Mz
Mz-
IRON HYDROGENASE
Ferredoxin- Ferredoxin+
FERREDOXIN
* TVAG_003900 1
* TVAG_399860 2
* TVAG_292710 4
TVAG_292711 5
TVAG_213140 3
TVAG_251200 6
TVAG_078730 7
?
PHOSPHOFRUCTOKINASE
TVAG_293770
TVAG_391760
TVAG_462920
TVAG_496160
CYTOSOL
Pyruvate
IRON HYDROGENASE
TVAG_037570 *
TVAG_182620 *
TVAG_310050 *
PYRUVATE: FERREDOXIN OXIDOREDUCTASE
TVAG_164890
TVAG_393850
TVAG_395550 *
ACETYL-CoA HYDROLASE
Acetyl-CoA
Acetate
Succinate
Succinyl-CoA
CoA
Pi
STK
ADENYLATE KINASE
2ADP
AMP + ATP
TVAG_489800
TVAG_072700
ADP
SUCCINYL-CoA SYNTHETASE
* TVAG_047890 α-chain (AP 33-3)
TVAG_259190 β-chain (AP 51-1)
TVAG_144730 β-chain (AP 51-2)
TVAG_165340 α-chain (AP 33-2)
TVAG_318670 α-chain (AP 33-1)
TVAG_183500 β-chain (AP 51-3)
TVAG_105770
TVAG_198110 *
TVAG_230580 *
TVAG_242960 *
TVAG_254890 *
TVAG_466790 *
DOWNREGULATED
UPREGULATED

Figure 6

Table 1

Accession Number	Manual annotation	Fold change	Datapoints	Metabolic pathway
TVAG_088220	Alanine aminotransferase-1	1.2	76	Aminoacid metabolism
TVAG_132440	Alanine aminotransferase-2	1.5	62	Aminoacid metabolism
TVAG_074600	Alanine aminotransferase-3	1.4	10	Aminoacid metabolism
TVAG_379550	Alanine aminotransferase-4	1.6	127	Aminoacid metabolism
TVAG_098820	Alanine aminotransferase-5	1.9	40	Aminoacid metabolism
TVAG_183850	Arginine deiminase - 1	2.1	19	Aminoacid metabolism
TVAG_467820	Arginine deiminase -3	2.0	23	Aminoacid metabolism
TVAG_344520	Arginine deiminase-2	1.7	4	Aminoacid metabolism
TVAG_177600	Glycine cleavage system H protein	2.1	61	Aminoacid metabolism
TVAG_272760	Glycine cleavage system, L protein	1.4	20	Aminoacid metabolism
TVAG_109540	Serine hydroxymethyltransferase	2.0	8	Aminoacid metabolism
TVAG_036010	A-type flavoprotein, TvFDP	1.0	319	Antioxidant / Detoxification
TVAG_040030	Iron sulfur flavoprotein -1	-10.4	2	Antioxidant / Detoxification
TVAG_154730	Iron sulfur flavoprotein -2	-6.3	8	Antioxidant / Detoxification
TVAG_410350	OsmC-1	1.6	66	Antioxidant / Detoxification
TVAG_412560	OsmC-2	2.5	14	Antioxidant / Detoxification
TVAG_064490	Rubrerythrin-1	-6.4	69	Antioxidant / Detoxification
TVAG_275660	Rubrerythrin-2	-17.9	2	Antioxidant / Detoxification
TVAG_049140	Superoxide dismutase	-5.3	16	Antioxidant / Detoxification
TVAG_055200	Thiol peroxidase	1.6	281	Antioxidant / Detoxification
TVAG_086470	Thioredoxin	2.0	66	Antioxidant / Detoxification
TVAG_418970	Thioredoxin	1.6	8	Antioxidant / Detoxification
TVAG_125500	Thioredoxin	1.9	2	Antioxidant / Detoxification
TVAG_385350	Thioredoxin	2.3	16	Antioxidant / Detoxification
TVAG_038090	Thioredoxin peroxidase-1	2.3	2	Antioxidant / Detoxification
TVAG_114310	Thioredoxin peroxidase-3	1.6	56	Antioxidant / Detoxification
TVAG_455310	Thioredoxin peroxidase-2	10.6	1	Antioxidant / Detoxification
TVAG_003900	Ferredoxin 1	-2.8	129	Electron transport
TVAG_399860	Ferredoxin 2	-5.9	28	Electron transport
TVAG_213140	Ferredoxin 3	1.9	10	Electron transport
TVAG_292710	Ferredoxin 4	-6.6	27	Electron transport
TVAG_292711	Ferredoxin 5	-3.6	1	Electron transport
TVAG_251200	Ferredoxin 6	1.6	11	Electron transport
TVAG_078730	Ferredoxin 7	1.3	22	Electron transport
TVAG_164890	Acetate:succinate CoA transferase-2	1.4	24	Energy metabolism
TVAG_395550	Acetate:succinate CoA transferase-3	-3.2	61	Energy metabolism
TVAG_393850	Acetate:succinate CoA transferase-4	6.0	2	Energy metabolism
TVAG_489800	Adenylate kinase-1	1.2	146	Energy metabolism
TVAG_072700	Adenylate kinase-2	7.6	2	Energy metabolism
TVAG_296220	Complex 1, 24 kDa subunit	-3.6	102	Energy metabolism
TVAG_133030	Complex1, 51kDa subunit	-2.9	275	Energy metabolism
TVAG_182620	Iron Hydrogenase-1	-2.3	45	Energy metabolism
TVAG_037570	Iron hydrogenase-2	-3.3	425	Energy metabolism
TVAG_310050	Iron hydrogenase-3	-9.0	19	Energy metabolism
TVAG_068130	Malic enzyme	-1.3	66	Energy metabolism
TVAG_267870	Malic enzyme	-1.5	12	Energy metabolism
TVAG_238830	Malic enzyme	1.2	340	Energy metabolism
TVAG_412220	Malic enzyme	-3.8	43	Energy metabolism
TVAG_340290	Malic enzyme	-2.1	809	Energy metabolism
TVAG_183790	Malic enzyme	-4.8	104	Energy metabolism
TVAG_416100	Malic enzyme	-2.4	34	Energy metabolism
TVAG_491670	Malic enzyme	-6.1	4	Energy metabolism
TVAG_293770	Phosphofructokinase TvPFK-1	1.5	252	Energy metabolism
TVAG_496160	Phosphofructokinase TvPFK-2	1.5	231	Energy metabolism
TVAG_462920	Phosphofructokinase TvPFK-3	1.6	416	Energy metabolism
TVAG_391760	Phosphofructokinase TvPFK-4	1.4	348	Energy metabolism
TVAG_198110	Pyruvate:ferredoxin oxidoreductase A	-5.4	411	Energy metabolism
TVAG_230580	Pyruvate:ferredoxin oxidoreductase BI	-37.4	8	Energy metabolism
TVAG_242960	Pyruvate:ferredoxin oxidoreductase, B-II	-13.5	162	Energy metabolism
TVAG_105770	pyruvate:ferredoxin oxidoreductase C	-1.6	2	Energy metabolism
TVAG_254890	Pyruvate:ferredoxin oxidoreductase E	-16.9	4	Energy metabolism
TVAG_466790	pyruvate:ferredoxin oxidoreductase F	-3.0	4	Energy metabolism
TVAG_318670	Succinyl Coa Synthetase	2.0	4	Energy metabolism
TVAG_165340	Succinyl-CoA synthetase alpha-chain	1.4	53	Energy metabolism
TVAG_047890	Succinyl-CoA synthetase alpha-chain	-2.3	54	Energy metabolism
TVAG_259190	Succinyl-CoA synthetase beta chain	-1.2	408	Energy metabolism
TVAG_183500	Succinyl-CoA synthetase beta chain	1.2	142	Energy metabolism
TVAG_144730	Succinyl-CoA synthetase beta-chain	1.6	227	Energy metabolism
TVAG_484900	S-adenosylmethionine synthetase	4.6	1	Energy metabolism

Table 1

TVAG_191660	Cpn10-1	1.6	64	Chaperones
TVAG_041340	Cpn10-2	1.2	39	Chaperones
TVAG_445730	Cpn10-3	1.7	25	Chaperones
TVAG_392320	Cpn10-4	1.5	38	Chaperones
TVAG_088050	Cpn60-1	1.5	25	Chaperones
TVAG_167250	Cpn60-2	1.2	64	Chaperones
TVAG_203620	Cpn60-3	-1.1	54	Chaperones
TVAG_381470	Hsp70 mitochondrial-type-1	1.1	5	Chaperones
TVAG_100490	Hsp70 mitochondrial-type-2	-1.3	1	Chaperones
TVAG_253630	Hsp70 mitochondrial-type-3	3.5	4	Chaperones
TVAG_237140	HSP70 Mitochondrial-type-4	-1.2	95	Chaperones
TVAG_340390	HSP70 Mitochondrial-type-5	1.5	118	Chaperones
TVAG_433130	HSP70 Mitochondrial-type-6	2.0	77	Chaperones
TVAG_305730	Jac1-1	-1.4	17	Chaperones
TVAG_262210	Jac1-2	1.1	6	Chaperones
TVAG_019190	Jac1-3	1.5	14	Chaperones
TVAG_182150	Frataxin-1	1.4	17	iron sulfur cluster assembly
TVAG_114560	Frataxin-2	1.4	2	iron sulfur cluster assembly
TVAG_027060	HydE-1	1.3	11	iron sulfur cluster assembly
TVAG_329200	HydE-2	2.7	9	iron sulfur cluster assembly
TVAG_205390	HydF	2.0	10	Iron sulfur cluster assembly
TVAG_469020	HydG-1	10.4	18	iron sulfur cluster assembly
TVAG_257780	HydG-2	-1.6	54	iron sulfur cluster assembly
TVAG_027170	Ind-1	1.6	36	Iron Sulfur cluster assembly
TVAG_076230	Ind-2	1.7	46	iron Sulfur cluster assembly
TVAG_217870	Ind-3	1.5	101	Iron sulfur cluster assembly
TVAG_277380	Ind-4	2.0	26	iron sulfur cluster assembly
TVAG_055320	IscA2-1	3.2	66	Iron Sulfur cluster assembly
TVAG_456770	IscA2-2	2.3	76	iron sulfur cluster assembly
TVAG_361540	IscA2-3	2.8	70	iron sulfur cluster assembly
TVAG_239660	IscS-2	1.6	129	Iron sulfur cluster assembly
TVAG_432650	IscU	1.1	28	iron sulfur cluster assembly
TVAG_242760	Isd11-1	2.2	74	Iron sulfur cluster assembly
TVAG_215080	Isd11-2	1.5	2	Iron sulfur cluster assembly
TVAG_182340	Mge (GrpE) -1	2.2	20	iron sulfur cluster assembly
TVAG_297650	Mge (GrpE) -2	1.7	73	Iron sulfur cluster assembly
TVAG_044500	Nfu-1.	3.1	25	iron sulfur cluster assembly
TVAG_008840	Nfu-2	3.2	63	iron sulfur cluster assembly
TVAG_451860	Nfu-3	4.7	56	iron sulfur cluster assembly
TVAG_146780	Nfu-4	8.7	46	iron sulfur cluster assembly
TVAG_119710	Hydrogenosomal processing peptidase alpha-subunit	1.5	31	Peptidases
TVAG_233350	Hydrogenosomal processing peptidase beta subunit	1.1	6	Peptidases
TVAG_461020	ABC transporter	-1.1	2	Protein translocation and maturation
TVAG_237680	ATP/ADP carrier-1, Hmp31. Integral polytopic protein	1.3	372	Protein translocation and maturation
TVAG_262210	ATP/ADP carrier-2	1.7	2	Protein translocation and maturation
TVAG_051820	ATP/ADP carrier-2	-1.9	217	Protein translocation and maturation
TVAG_190830	C-tail-2	1.4	7	Protein translocation and maturation
TVAG_272350	C-tail-4	1.1	8	Protein translocation and maturation
TVAG_137270	C-tail-6	1.8	38	Protein translocation and maturation
TVAG_277930	C-tail-7	1.2	28	Protein translocation and maturation
TVAG_283120	C-tail-8	1.4	41	Protein translocation and maturation
TVAG_369980	C-tail-10	1.6	38	Protein translocation and maturation
TVAG_393390	C-tail-11	-1.5	8	Protein translocation and maturation
TVAG_211970	C-tail-12	-1.4	8	Protein translocation and maturation
TVAG_104250	Hmp35 -2	-2.1	200	Protein translocation and maturation
TVAG_031860	Hmp-36-1	1.2	146	Protein translocation and maturation
TVAG_216170	Hmp-36-2	1.3	203	Protein translocation and maturation
TVAG_470110	Pam16	1.8	14	Protein translocation and maturation
TVAG_146920	Porin-1	-1.1	2	Protein translocation and maturation
TVAG_178100	SAM50	1.3	8	Protein translocation and maturation
TVAG_287510	small Tim9-10A	1.5	3	Protein translocation and maturation
TVAG_026080	small Tim9-10B	1.5	8	Protein translocation and maturation
TVAG_399830	TIM 8	1.3	2	Protein translocation and maturation
TVAG_260640	Tim10-1	-1.1	2	Protein translocation and maturation
TVAG_061900	Tim17/22/23B	1.3	28	Protein translocation and maturation
TVAG_370860	Tim17/22/23C	2.1	6	Protein translocation and maturation
TVAG_447580	Tim17-like	1.4	6	Protein translocation and maturation
TVAG_008790	Tim44	1.8	20	Protein translocation and maturation
TVAG_399510	Tom40-1	1.0	2	Protein translocation and maturation
TVAG_450220	Tom40-3	1.2	10	Protein translocation and maturation
TVAG_195900	Tom40-6	1.6	19	Protein translocation and maturation
TVAG_225560	Unknown. Integral monotopic single spanning protein	1.4	4	Protein translocation and maturation
TVAG_423530	Unknown. Integral monotopic single spanning protein	1.7	27	Protein translocation and maturation
TVAG_455090	Unknown. Integral polytopic protein	-1.6	176	Protein translocation and maturation
TVAG_440200	Unknown. Integral polytopic protein	1.4	178	Protein translocation and maturation
TVAG_136450	Unknown. Integral polytopic protein	1.7	2	Protein translocation and maturation
TVAG_206500	Hybrid-cluster protein-1	-1.1	139	Unknown function
TVAG_336320	Hybrid-cluster protein-2	1.1	161	Unknown function

Table 2

UPREGULATED			
Accession Number	**Manual annotation**	**Fold change**	**Metabolic pathway**
TVAG_183850	Arginine deiminase - 1	2.1	Aminoacid metabolism
TVAG_467820	Arginine deiminase -3	2.0	Aminoacid metabolism
TVAG_177600	Glycine cleavage system H protein	2.1	Aminoacid metabolism
TVAG_109540	Serine hydroxymethyltransferase	2.0	Aminoacid metabolism
TVAG_412560	OsmC-2	2.5	Antioxidant / Detoxification
TVAG_086470	Thioredoxin	2.0	Antioxidant / Detoxification
TVAG_385350	Thioredoxin	2.3	Antioxidant / Detoxification
TVAG_318670	Succinyl Coa Synthetase	2.0	Energy metabolism
TVAG_253630	HSP70	3.5	Chaperones
TVAG_433130	HSP70	2.0	Chaperones
TVAG_329200	HydE	2.7	iron sulfur cluster assembly
TVAG_205390	HydF	2.0	Iron sulfur cluster assembly
TVAG_469020	HydG	10.4	iron sulfur cluster assembly
TVAG_277380	Ind-4 (P-Loop ATPase-3)	2.0	iron sulfur cluster assembly
TVAG_055320	IscA2-1	3.2	Iron Sulfur cluster assembly
TVAG_456770	IscA2-2	2.3	iron sulfur cluster assembly
TVAG_361540	IscA2-3	2.8	iron sulfur cluster assembly
TVAG_242760	Isd11	2.2	Iron sulfur cluster assembly
TVAG_182340	Mge (GrpE)-1	2.2	iron sulfur cluster assembly
TVAG_044500	Nfu-1.	3.1	iron sulfur cluster assembly
TVAG_008840	Nfu-2	3.2	iron sulfur cluster assembly
TVAG_451860	Nfu-3	4.7	iron sulfur cluster assembly
TVAG_146780	Nfu-4	8.7	iron sulfur cluster assembly
TVAG_370860	Tim17/22/23C	2.1	Protein translocation and maturation

DOWNREGULATED			
Accession Number	**Manual annotation**	**Fold change**	**Metabolic pathway**
TVAG_154730	Iron sulfur flavoprotein	-6.3	Antioxidant / Detoxification
TVAG_064490	Rubrerythrin	-6.4	Antioxidant / Detoxification
TVAG_049140	Superoxide dismutase	-5.3	Antioxidant / Detoxification
TVAG_003900	Ferredoxin 1	-2.8	Electron transport
TVAG_399860	Ferredoxin 2	-5.9	Electron transport
TVAG_292710	Ferredoxin 4	-6.6	Electron transport
TVAG_395550	Acetate:succinate CoA transferase	-3.2	Energy metabolism
TVAG_296220	Complex 1, 24 kDa subunit	-3.6	Energy metabolism
TVAG_133030	Complex1, 51kDa subunit	-2.9	Energy metabolism
TVAG_182620	Iron Hydrogenase-1	-2.3	Energy metabolism
TVAG_037570	Iron hydrogenase-2	-3.3	Energy metabolism
TVAG_310050	Iron hydrogenase-3	-9.0	Energy metabolism
TVAG_412220	Malic enzyme D	-3.8	Energy metabolism
TVAG_340290	Malic enzyme H	-2.1	Energy metabolism
TVAG_183790	Malic enzyme	-4.8	Energy metabolism
TVAG_416100	Malic enzyme	-2.4	Energy metabolism
TVAG_491670	Malic enzyme	-6.1	Energy metabolism
TVAG_430830	Phosphofructokinase	-4.0	Energy metabolism
TVAG_198110	Pyruvate:ferredoxin oxidoreductase A	-5.4	Energy metabolism
TVAG_230580	Pyruvate:ferredoxin oxidoreductase BI	-37.4	Energy metabolism
TVAG_242960	Pyruvate:ferredoxin oxidoreductase, B-II	-13.5	Energy metabolism
TVAG_254890	Pyruvate:ferredoxin oxidoreductase E	-16.9	Energy metabolism
TVAG_466790	pyruvate:ferredoxin oxidoreductase F	-3.0	Energy metabolism
TVAG_047890	Succinyl-CoA synthetase alpha-chain	-2.3	Energy metabolism
TVAG_104250	Hmp35 -2	-2.1	Protein translocation and maturation